Seismic Activity Associated with a Probable Submarine Eruption near Tristan da Cunha, July 2004–July 2006

Aoife O'Mongain, Lars Ottemoller, Brian Baptie, David Galloway, and David Booth
British Geological Survey

INTRODUCTION

The remote South Atlantic island of Tristan da Cunha (hereafter abbreviated to "Tristan") is a large oceanic shield volcano rising more than 5,500 m from the sea floor to an altitude of 2,060 m above sea level. Tristan along with the islands Inaccessible and Nightingale and a number of smaller islets forms the Tristan da Cunha group (figure 1), which lies on a submarine plateau approximately 200 km east of the Mid-Atlantic Ridge near its junction with the Walvis Ridge (Morgan 1971; Fairhead and Wilson 2005). The group is believed to represent the surface volcanic expression of a mantle plume or hotspot. The most recent eruption on Tristan was in 1961–62 (Baker *et al* 1964) and was preceded by two months of tremors felt by the population.

Earthquakes along the Mid-Atlantic Ridge dominate the regional seismicity of the area (figure 1). Recently, Haxel and Dziak (2005) detected low magnitude ($M \leq 3$) earthquakes attributed to submarine volcanic activity on the Walvis Ridge, about 800 km northwest of Tristan, through observations of *T*-phases recorded on hydrophones in 2002 and 2003. We know very little about the local seismicity of the Tristan group itself because of the large distances to the nearest seismometers. However, in March 2004 the Comprehensive Nuclear-Test-Ban Treaty Organization/International Monitoring System (CTBTO/IMS) installed two seismic stations on Tristan, approximately 5 km apart, to enable hydroacoustic wave monitoring through the detection of seismic *T*-phases for nuclear test-ban treaty verification purposes. The locations of these sta-

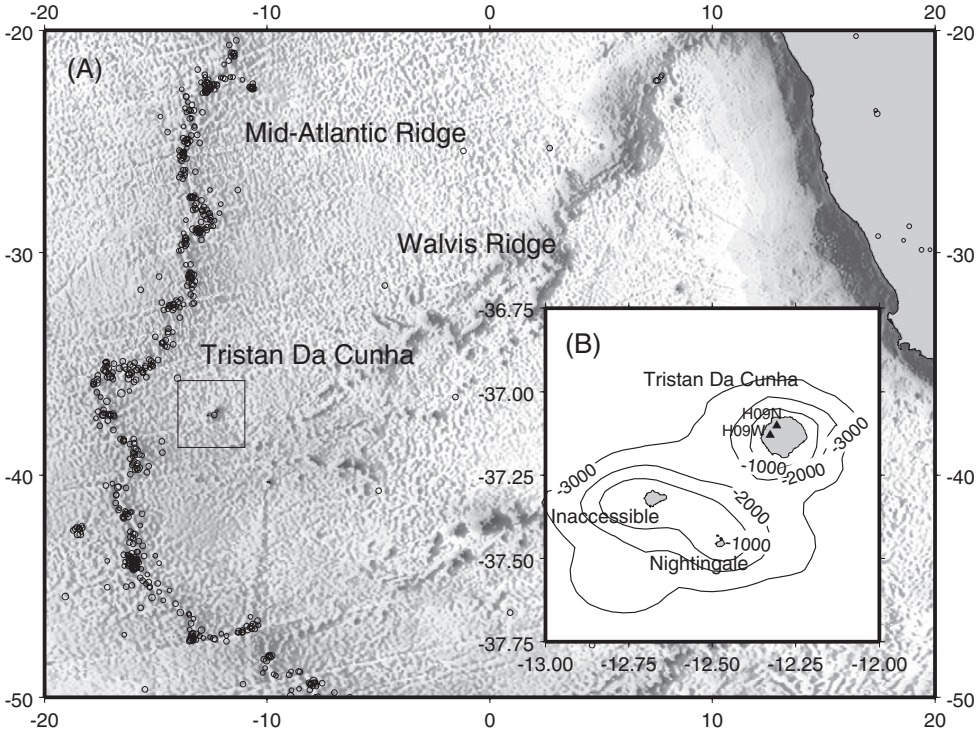

▲ **Figure 1.** (A) Bathymetry of the South Atlantic from ETOPO2 (Smith and Sandwell 1997). Earthquakes from the NEIC database from 1973 to present are shown as open circles. (B) Inset shows the islands of the Tristan da Cunha archipelago and the locations of the two IMS stations H09N and H09W.

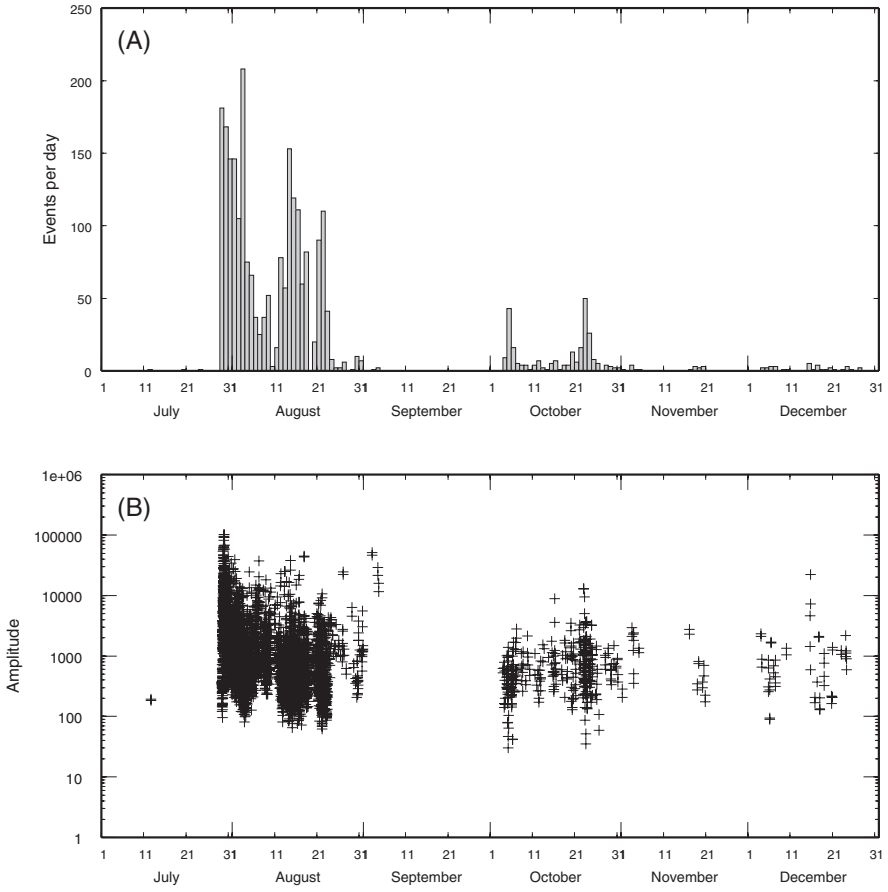

▲ **Figure 2.** Number of events per day (A) and maximum displacement *S*-wave amplitudes (nm) (B) for the period from 01 July 2004 to 31 December 2004 for station H09W. Note there is a gap in our analysis for September 2004.

tions, H09W and H09N, are shown in figure 1. Each station is equipped with a three-component short-period seismometer, and data are recorded at 100 samples per second. At the same time, the Incorporated Research Institutions for Seismology (IRIS) installed a broadband STS-2 seismometer (TRIS) with a sample rate of 20 samples per second, colocated with H09N.

A sequence of earthquakes starting in July 2004 caused widespread alarm among the local population. The largest of the earthquakes was detected by the Global Seismograph Network and assigned a magnitude of 4.8 m_b according to the National Earthquake Information Center (NEIC). Only eight other events (listed in table 1) were detected at stations outside Tristan, which means that most events have to be located with only the two local stations. A rapid hazard assessment (Hards 2004) found no evidence of recent volcanic activity on Tristan itself, but the appearance of fresh pumice on some of the island's beaches suggested the occurrence of a recent submarine eruption. This observation leads us to the assumption that the seismicity described here is related to volcanic activity.

From October 2004 to July 2006, we used near–real-time data from the CTBTO and IRIS stations on Tristan to monitor seismic activity on Tristan and assess possible volcanic hazard. Additional continuous data from July to August 2004 was provided by the IMS for retrospective data processing. Our data analysis has a gap in September 2004 because retrospective analysis was restricted to July and August 2004 and real-time monitoring began in October 2006. Both data sets were processed using a simple STA/LTA detection algorithm to detect seismic events. Detected events were then carefully reviewed to discriminate spurious signals. Where possible, we picked *P*- and *S*-wave arrival times at each station along with event back-azimuth determined from *P*-wave polarization analysis. We obtained a catalog of earthquake activity for the time period July 2004 to July 2006 that contains about 2,500 events.

In this paper, we present the results of our analysis of data from the two local seismic stations on Tristan between July 2004 and July 2006. Our main objective is to determine event locations using data from these two stations. We also describe temporal changes in event occurrence and size. Finally, we discuss the results and the implications for both seismic and volcanic hazard on Tristan.

OBSERVED SEISMIC ACTIVITY

Based on the catalog of local seismicity at Tristan, we examine the temporal distribution of the number of events per day and the maximum *S*-wave amplitudes on station H09W of the 2,566 earthquakes detected from 1 July 2004 to 31 December 2004 (figure 2). Activity appears to consist of periods of intense earthquake activity that stand out clearly as vertical bands on

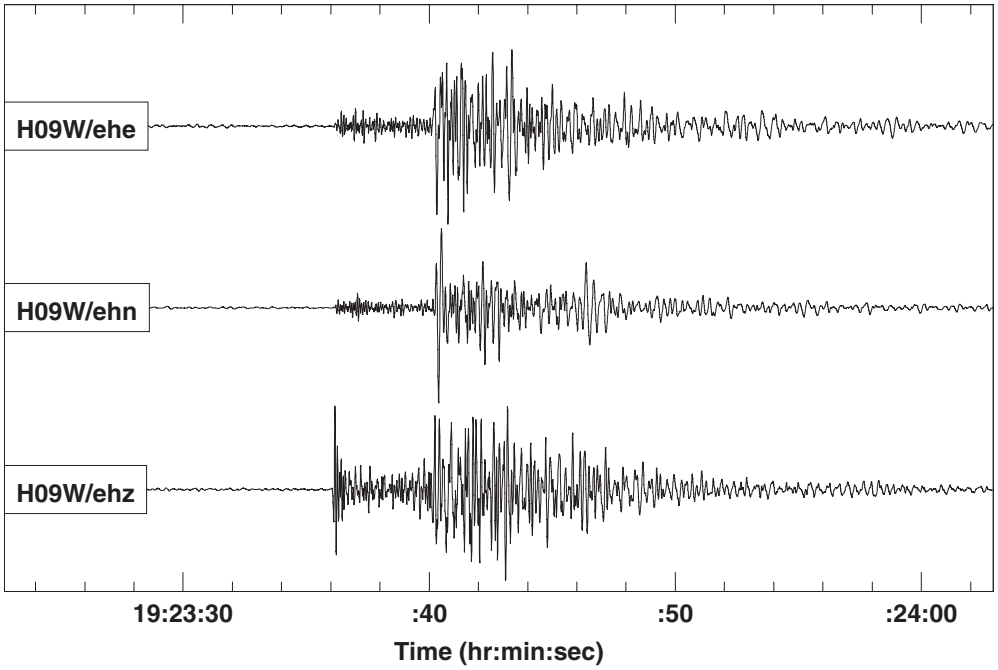

▲ **Figure 3.** Seismograms recorded at station H09W for an earthquake on 5 August 2004 at 19:23 UTC.

the amplitude plot. The first earthquakes start abruptly at 11:33 on 29 July and activity remains at a very high level until around 06:00 on 30 July, with a total of more than 300 discrete earthquakes. There is no precursory activity in the period leading up to 29 July. Subsequent activity is less intense, although the number of events per day reaches its peak on 3 August. This then decreases until 10 August when it starts to increase again, peaking for a second time around 20 August. After the end of August the number of events per day falls to less than 10 on average, and by March 2005 (not shown) the number of events has returned to a low background level.

The event amplitudes in figure 2 initially show a large range that varies by three orders of magnitude. However, after the initial swarm on 29–30 July, amplitudes generally decrease with time, with the exception of occasional large events. Thirty-two of the earthquakes in this time period had a magnitude greater than 4.0 M_L. Nine of these events were detected outside Tristan and were located using observations from the global network.

Figure 3 shows the three components of ground motion recorded at station H09W for an earthquake on 5 August 2004 at 19:23 UTC. The signal to noise ratio on station H09W is significantly higher than those at either H09N or TRIS. The signals show all the characteristics of classical tectonic earthquakes with impulsive *P* arrivals followed by clear *S* arrivals. Therefore we attribute the events to brittle failure within the crust. Following Lahr *et al* (1994) we have classified the events as volcano-tectonic (VT) earthquakes.

The buildup of seismicity on 29–30 July is examined in detail in figure 4. There is a clear increase in both the number of events per hour and the amplitude of individual events with time. This peaks between 22:21 on 29 July and 01:05 on 30 July with four earthquakes in the range 4.7–4.8 m_b. After this both the number of events per hour and their amplitudes generally decrease, but a number of larger events still occur. This trend shows strong similarities to earthquake swarms observed in volcanic regions, rather than a typical mainshock-aftershock sequence following a large tectonic earthquake.

EARTHQUAKE LOCATION

The accuracy of any earthquake location estimate is restricted by sparse data, as in the case of Tristan with only two stations. The minimum requirement to locate individual events recorded on only two stations is three phase readings and one azimuth reading. However, based on these, the error in each earthquake location is of the order of 50 km. Rather than locate the earthquakes individually, we use a different approach to determine a location estimate for all events. Because we believe that the events are related to near-surface volcanic activity, we fixed the depth of all events to 3 km.

For all detected events with appropriate signal-to-noise ratio we measure *P*-wave arrival times at each station and calculate the relative time difference in *P*-wave arrivals between the two stations. For a given *P*-wave incidence angle we calculate theoretical *P*-wave delay times between the two stations as a function of back-azimuth (*e.g.*, Schweizer *et al.* 2002). This can then be compared with the observed time differences to provide an estimate of the actual event back-azimuth.

The time difference between the *P*-wave arrival and the *S*-wave arrival at each station (*S-P* time) provides an estimate of the distance traveled from the source, depending on the velocity model. We use an oceanic velocity model derived from the model published for Ascension Island (Evangelidis *et al.* 2004). Our model consists of two layers above the Moho of 5 km

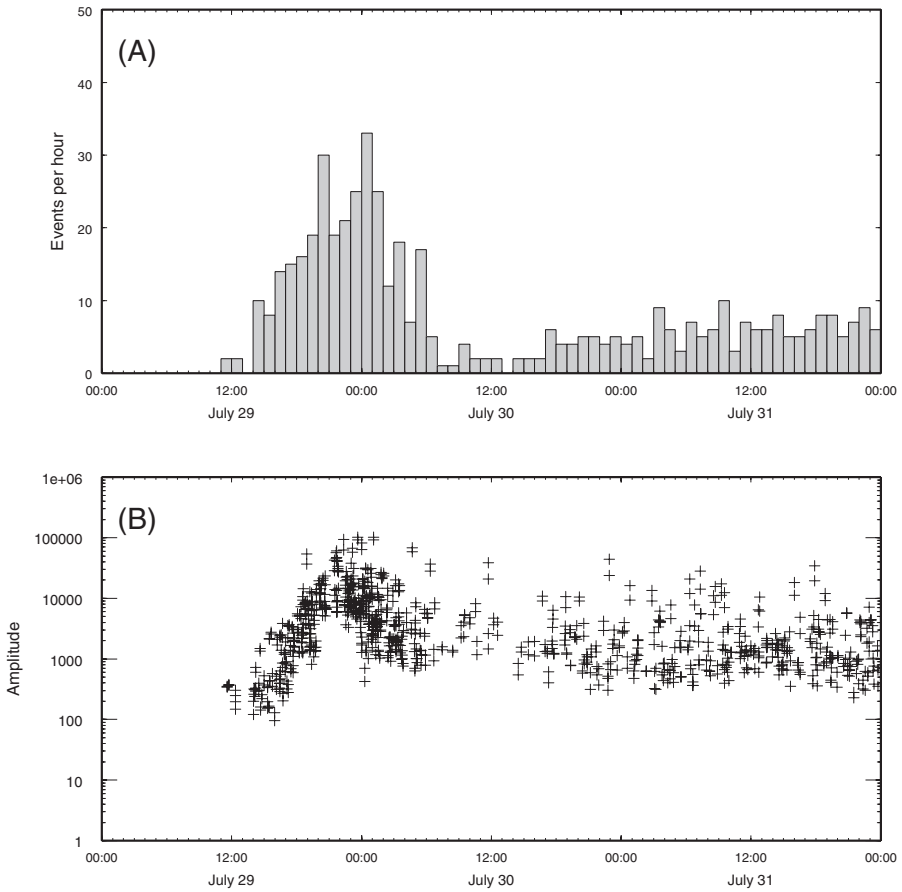

▲ **Figure 4.** Number of events per hour (A) and maximum displacement *S*-wave amplitudes (nm) (B) for the period from 28 July 2004 to 31 July 2004 for station H09W.

thickness and *P* velocities of 6.1 and 7.1 km/s, respectively, and a V_p/V_s ratio of 1.73. Mantle velocity is assumed to be 8 km/s.

Finally, we estimate the event back-azimuth from the *P*-wave arrivals recorded at station H09W using the polarization analysis method of Roberts *et al.* (1989). The errors involved in this method are relatively large, even for good signal-to-noise ratios. However, by determining the azimuth this way, it is possible to choose which of the two directions determined from the *P*-wave delay times is the true one.

The measured time differences in the *P*-wave arrivals between stations H09N and H09W are shown in figure 5A. The *P* waves for all events arrive first at H09W, indicating that the earthquake source is nearer H09W than H09N. The delay time for 90% of the events is between 0.28 and 0.51 sec, showing that the waves are coming from a similar direction. More scatter in the times might suggest that the earthquakes are at a range of azimuths and not from a specific direction. The average time differences in the *P*-wave arrivals between H09N and H09W of 0.38 are consistent with our modeling of the first arrivals as refracted waves. This suggests that the events are beyond the critical distance and certainly not directly below Tristan.

Figure 5B shows *P*-wave delay time as a function of back-azimuth calculated using a *P*-wave incidence angle of 59° corresponding to a mantle refracted wave. The observed time delay of 0.28–0.51 sec corresponds to back-azimuths of either 151°–195° or 222°–266°. *S-P* times for all detected events are shown in figure 5C. Ninety percent of the *S-P* times lie within the range 3.87–5.46 sec with a mean of 4.66 sec. Based on our assumed velocity model, this corresponds to epicentral distances in the range 37.6–53.0 km, with a mean of 45.3 km. Figure 5D shows event back-azimuths calculated using *P*-wave polarization analysis. The calculated azimuths show a scatter of the order of around 100°; however, it is clear that the events lie to the southeast rather then the southwest of Tristan. This observation allows us to discriminate between the two possible azimuths from the *P*-wave delay times, giving a final azimuth estimate of 151°–195°.

We also located the largest events that were detected on Global Climate Observing System (GCOS) Surface Network (GSN) stations outside Tristan by using *P* and *S* arrivals on the Tristan stations, and the azimuth reading and *P*-arrival times from GSN stations (table 1). At a fixed depth of 3 km, the formal horizontal errors in event location are of the order of 10 km. We also determined m_b at teleseismic distances where possible. Out of the four largest events with an m_b of either 4.7 or 4.8, only the one at 22:21 on 29 July was detected by the IMS and NEIC. This is also the only event where we were able to pick arrival times at teleseismic distances at more than one sta-

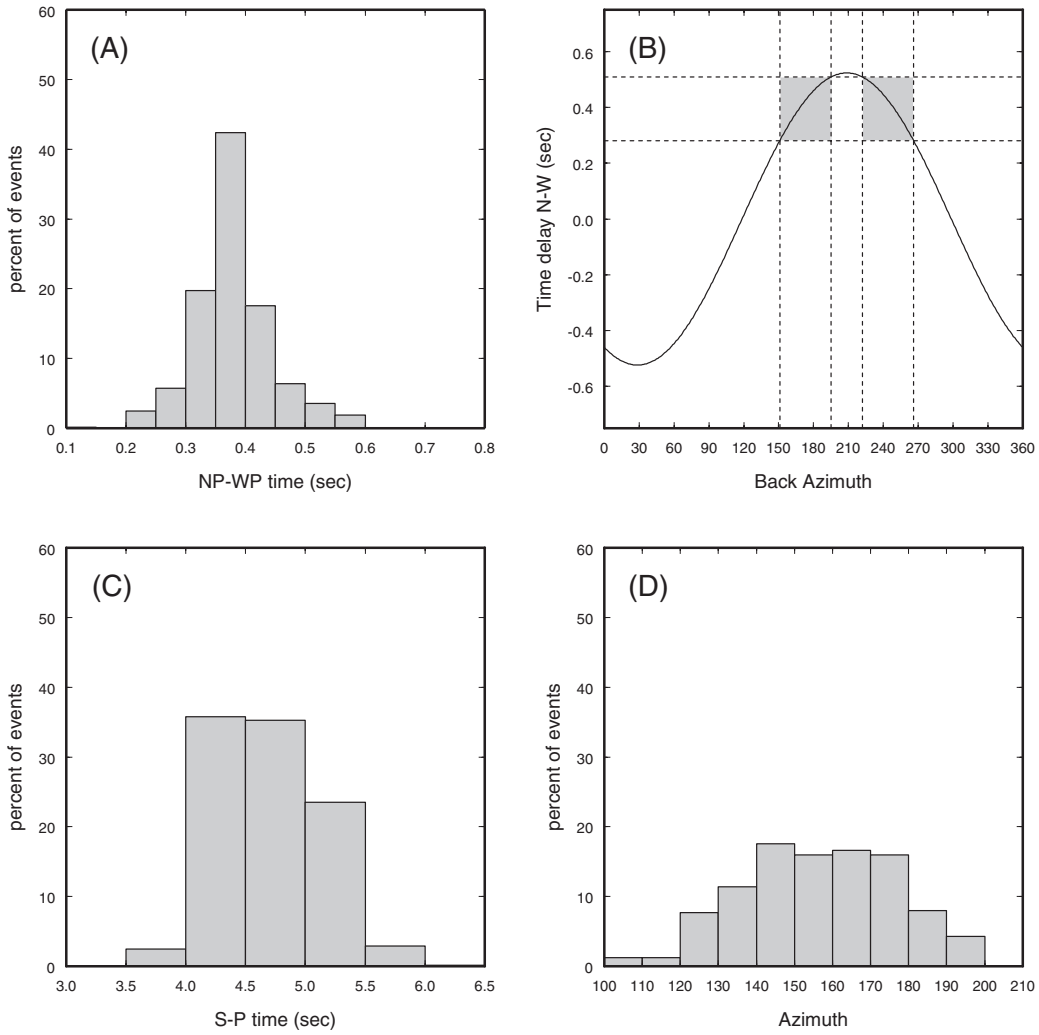

▲ **Figure 5.** (A) *P*-wave arrival time difference between stations H09W and H09N. (B) Time delay (North P – West P) as function of back-azimuth for station H09W assuming an incidence angle of 59° corresponding to a mantle refracted wave. (C) *S-P* arrival times for all events. (D) Measured azimuths from H09W for all located events.

tion. The only station that picked up the other events is QSPA, which is located at the South Pole and known to be a quiet site. It is not clear why some of the events with even greater magnitude than the one at 22:21 are not detected by other stations, but it could be related to source characteristics or event depth.

These results allow us to draw a confidence ellipse for all events, where the 90% range for event back-azimuth and *S-P* time defines the lengths of the major and minor axes, respectively. The orientation of the ellipse is defined by the mean back-azimuth value. This 90% confidence ellipse is shown in figure 6. The area of the ellipse is just more than 400 km^2. The ellipse covers the locations of the largest events that also were detected by global stations, considering uncertainty.

MAGNITUDE AND B-VALUE

We calculate local magnitudes (M_L) for all earthquakes with amplitude readings using the relationship given by Hutton and Boore (1987). We use the maximum amplitude reading for each event and the average epicentral distance of 45 km to calculate M_L. We then examine the relationship between earthquake size and frequency of occurrence by calculating the *b*-value for all earthquakes with amplitude readings from July 2004 to July 2006. Data completeness is reached at a magnitude of 2.6 M_L, which gives an indication of the threshold of our detection capability. The least squares *b*-value we obtain is 1.19, which is higher than expected for typical tectonic earthquakes. A *b*-value greater than 1 indicates the lack of the largest magnitude events expected given the observed number of smaller events. We find no evidence of a change in *b*-value throughout the monitoring period. The most intense sequence of events in July–August 2004 exhibit a magnitude-frequency distribution (*b*-value) of 1.17.

DISCUSSION

We have presented the first analysis of local seismicity using instrumental data from Tristan da Cunha. An abrupt increase

TABLE 1
Parameters of the nine largest events that were detected by at least one station outside Tristan. The event on 29 July 2004 at 22:21 was detected by nine stations outside Tristan; this was the only event that was included in the IMS and NEIC bulletins. These locations also are given in table 1. All other events were detected by only one station outside Tristan.

Year	Month	Day	HrMi	Sec	Latitude	Longitude	Depth (fixed)	RMS	M_L	m_b
2004	7	29	1856	48.0	–37.267	–11.934	3.0	0.4	4.4	
2004	7	29	2138	30.9	–37.428	–12.216	3.0	0.1	4.4	
2004	7	29	2140	55.7	–37.296	–11.988	3.0	0.2	4.3	
2004	7	29	2144	32.1	–37.532	–12.211	3.0	0.7	4.5	
2004	7	29	2221	12.5	–37.450	–12.334	3.0	0.5	4.6	4.7
	NEIC		2221	06.9	–37.309	–12.371	18.2	1.23		4.8
	IMS		2221	04.6	–37.198	–12.343	0.0 (F)			4.2
2004	7	29	2339	48.7	–37.400	–12.104	3.0	0.1	4.7	4.8
2004	7	30	0000	43.7	–37.389	–12.080	3.0	0.2	4.6	4.8
2004	7	30	0105	20.8	–37.445	–12.325	3.0	0.3	4.7	4.8
2004	7	30	0441	35.2	–37.444	–12.284	3.0	0.1	4.5	

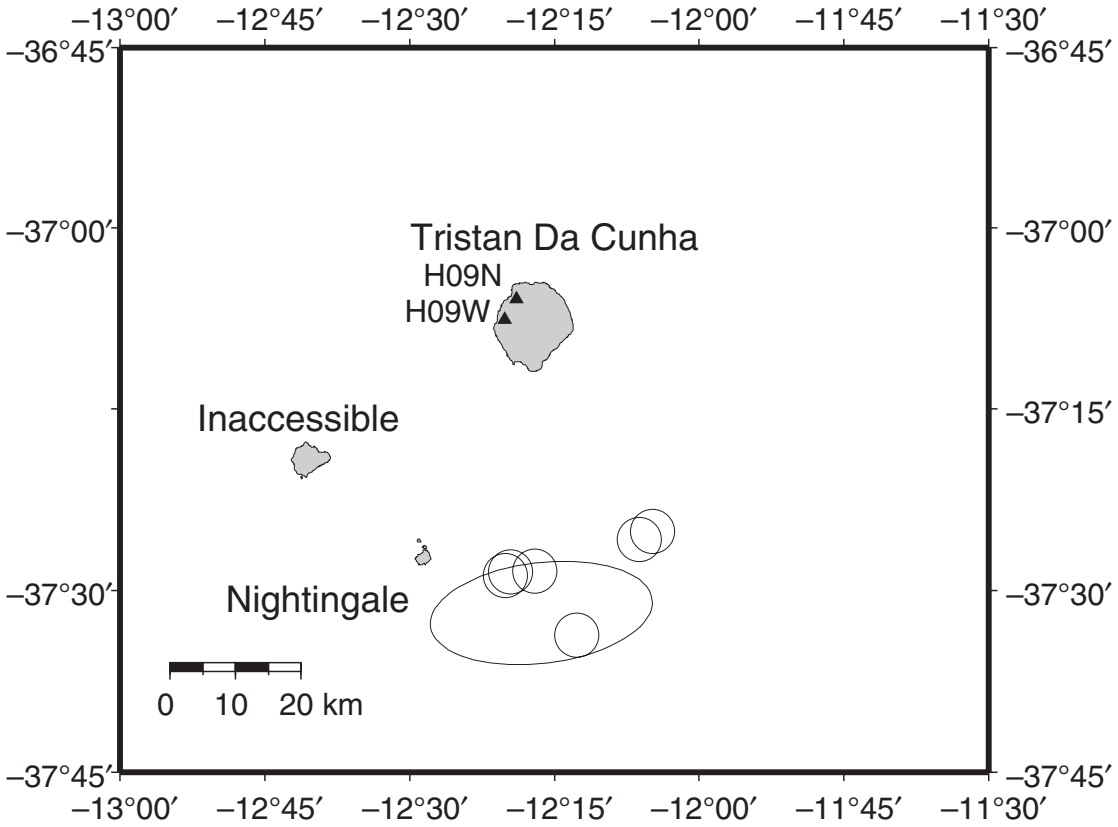

▲ **Figure 6.** Ninety percent confidence ellipse derived from *P*-wave time differences, *S-P* times, and *P*-wave polarization analysis showing the most likely location area for events between July 2004 and July 2006. The 90% range for event back-azimuth and *S-P* time defines the lengths of the major and minor axes, respectively. The orientation of the ellipse is defined by the mean back-azimuth. The open circles show locations of the nine largest local events calculated using GSN and IMS data.

in local seismic activity was observed on 29 July 2004 with a number of bands of intense earthquake activity over the following few days. Earthquakes continued to occur in the following months, and activity remained at an elevated level until early 2005. After this time the activity returned to what we assume is the background level. Monitoring has continued to the time of this writing and no similar activity has been observed. The absence of events near Tristan in global catalogs merely reflects the previously high detection threshold in the region. It remains to be seen if such earthquake activity happens regularly or whether the July/August 2004 episode is an isolated incident.

Although the recorded seismograms show all the characteristics of classical tectonic earthquakes with impulsive *P* arrivals and clear *S* arrivals, the temporal variation of both event numbers and amplitudes is more in keeping with the earthquake swarms observed in volcanic regions than with a typical mainshock-aftershock sequence. The observation of pumice on Tristan is probably the main argument for assuming that the events are related to volcanic activity. The most favored explanation for high *b*-values is a weak crust incapable of sustaining high strain and heterogeneous stress (Lay and Wallace 1995). In this case the high *b*-value may suggest that the stresses causing the observed seismicity are a result of volcanic rather than tectonic activity.

The distinctive increase in both number of events and their amplitudes with time on 29 July 2004 can be interpreted as strong evidence for volcanic activity, with magma forcing its way up through the crust resulting in brittle failure of the surrounding rock. Depth estimates could provide further evidence, but we were unable to resolve event depths with the data available. The largest earthquakes of the entire sequence occurred between 22:21 on 29 July and 01:05 on 30 July, perhaps signifying the onset of surface extrusion.

The steady increase in event numbers and amplitudes observed on 29–30 July 2004 also has important consequences for future monitoring. Similar trends might offer the possibility of forecasting any future eruption and providing a warning to the islanders. However, there is no guarantee that any future eruption will follow the same pattern. Because the islanders would be unlikely to feel smaller events occurring at the start of any future earthquake swarm, continued analysis of instrumental data is essential. Most critical to the islanders is to determine whether seismic events are beneath Tristan, which may indicate high risk, or at a reasonable distance, which would indicate low risk.

Despite having data from only two seismograph stations we were able to use relative *P*-wave arrival times, *S-P* arrival times and azimuth measurements to estimate earthquake locations. Our interpretation suggests that the source is not deep and directly beneath the island but between 37–53 km SSE from the stations at a relatively shallow depth.

The offshore location is consistent with the observations of Hards (2004), who examined pumice that was found floating near Tristan in August 2004 and washed up on some of its beaches. Baker *et al* (1964) display a map of the local bathymetry based on a British Admiralty chart. It shows a submarine seamount located 12 km NE of Nightingale Island and 26 km south of Tristan. This is the only notable feature on the map that might be associated with previous eruptive activity and is located close to the area where we have located the seismic activity.

Prior to the submarine eruption on the flank of the Tristan volcano discussed here, the last eruption was in 1961 (and very close to the settlement), which is very recent in geological terms. The volcano must certainly be categorized as active, and we suggest that continued monitoring is necessary for the foreseeable future to determine what activity constitutes normal "background" seismic behavior for the island and what is unusual activity that might precede an eruption.

CONCLUSIONS

In July 2004, earthquake activity felt on the South Atlantic island of Tristan da Cunha caused widespread alarm, as seismic activity had preceded a destructive volcanic eruption in 1961. Analysis of data from two seismograph stations on the island shows a dramatic increase in earthquake activity beginning on 29 July 2004, with more than 2,000 local earthquakes detected between July and December 2004. Furthermore, we find that the initial earthquake activity shows a consistent increase in amplitude with time, culminating in four magnitude 4.7–4.8 m_b earthquakes on 29–30 July, the largest detected over the monitoring period. There is no evidence of precursory activity in the period before 29 July 2004. We estimate the location of the earthquakes using the relative *P*-wave arrival times at the two stations, *S-P* arrival times, and azimuths determined from *P*-wave polarization analysis. Our analysis suggests that, despite the relatively large errors associated with sparse data, all the events are located between 37 and 53 km SSE of the island and are probably associated with an offshore submarine volcanic eruption. The July 2004 swarm, and its abrupt onset, is a reminder that this volcanic complex is still active, and there is clearly a potential for further large earthquakes and swarm earthquakes associated with volcanic activity. Warning times before an eruption could be short, so seismic monitoring is essential for accurate hazard assessment.

ACKNOWLEDGMENTS

The authors gratefully acknowledge the services provided by the Comprehensive Nuclear-Test-Ban Treaty Organization (CTBTO) in supplying data from its International Monitoring System (IMS) stations on Tristan da Cunha. In particular, we thank Rod Stewart, Mubu Singute Mubu, and their colleagues. We also thank Peter Marshall and Peter Bartholomew at Atomic Weapons Establishment Blacknest for providing the necessary authorization to receive the data. The facilities of the IRIS Data Management System, and specifically the IRIS Data Management Centre, were used for access to waveform and metadata required in this study. This work is published with the permission of the Executive Director of the British Geological Survey (NERC).

REFERENCES

Baker, P E, I. Gass, P. G. Harris, and R. W. Le Maitre (1964). The volcanological report of the Royal Society Expedition to Tristan da Cunha 1962. *Philosophical Transactions of the Royal Society* **256**, 439–578.

Evangelidis, C. P., T. A. Minshull, and T. J. Henstock (2004). Three-dimensional crustal structure of Ascension Island from active source seismic tomography. *Geophysical Journal International* **159**, 311–325.

Fairhead, J. D., and B. M. Wilson (2005). Plate tectonic processes in the South Atlantic Ocean: Do we need deep mantle plumes? In *Plates, Plumes and Paradigms*, ed. G. R. Foulger, J. H. Natland, D. C. Presnall, and D. L. Anderson, 537–553. Geological Society of America Special Paper 388, Boulder, CO: Geological Society of America.

Hards, V. (2004). Assessment of volcanic activity in the wake of the seismic episode of 29/30 July 2004 on Tristan da Cunha, South Atlantic Ocean. British Geological Survey Commissioned Report CR/04/235, 20 pp.

Haxel, J. H., and R. P. Dziak (2005). Evidence of explosive seafloor volcanic activity from the Walvis Ridge, South Atlantic Ocean. *Geophysical Research Letters* **32**, L13609.

Hutton, L. K., and D. Boore (1987). The M_L Scale in Southern California. *Bulletin of the Seismological Society of America* **77**, 2,074–2,094.

Lahr, J. C., B. A. Chouet, C. D. Stephens, J. A. Power, and R. A. Page (1994). Earthquake classification, location and error analysis in a volcanic environment. *Journal of Volcanology and Geothermal Research* **62**, 137–151.

Lay, T., and T. C. Wallace (1995). *Modern Global Seismology*. San Diego: Academic Press.

Morgan, W. J. (1971). Convection plumes in the lower mantle *Nature* **230**, 42–43.

Roberts, R G., A. Christoffersson, and F. Cassidy (1989). Real-time event detection, phase identification and source location estimation using single station three-component seismic data. *Geophysical Journal* **97**, 471–480.

Schweizer, J., J. Fyen, S. Mykkeltveit, and T. Kværne (2002). Seismic arrays. In *IASPEI—New Manual of Seismological Observatory Practice*, ed. P Bormann, chapter 9. Potsdam, Germany: GeoForschungsZentrum.

Smith, W. H. F., and D. T. Sandwell (1997). Global sea floor topography from satellite altimetry and ship depth soundings. *Science* **277**, 5,334.

British Geological Survey
Murchison House, West Mains Road
Edinburgh, EH9 3LA, United Kingdom
bbap@bgs.ac.uk
(B.B.)